

## **CHAPTER-7**

# **DIAGENESIS OF SIWALIK SEDIMENTS AND ITS EFFECT ON STABLE ISOTOPES**

## 7.1 Introduction

Freshly deposited sediments are commonly unconsolidated, with relatively low bulk density and high permeability and if accumulated under water, contain substantial amount of water. Subsequently, while being buried under younger sediments, the older sediments progressively lose water and become denser and lithified. All the changes involved in such a process is collectively termed diagenesis (Gerhard, 2000). Diagenesis can be of two types: mechanical and chemical. Mechanical diagenesis results from vertical stresses caused by overburden of younger sediments and, in some cases, by additional stresses due to tectonic movements. It expels pore water and leads to a rearrangement of the sediment particles. Chemical diagenesis involves dissolution and re-crystallization of primary sediment particles as well as precipitation of cement in pore space. Dissolution and cementation may take place at different depth levels within the sediments. The effects of mechanical and chemical diagenesis in various sediment types are quite complex but some issues can be investigated using a variety of proxies.

Siwalik sediments of Himalayan foothills were deposited continuously by various rivers in the foothills of Himalaya for last 20 Myr (Johnson et al., 1985) and provide an excellent opportunity to study diagenetic changes in fluvial sediments over a specified time. As a whole, the Siwalik sediments are characterized by coarsening upwards reflecting increase in energy levels for sediment transport with time. The lower and middle Siwalik sediments consist of alternation of sandstone and mudstone beds while upper Siwalik is mostly characterized by alternation of conglomerate and mudstone beds with occasional lenses of sandstone in-between. Compositionally, the sandstone is lithic arenite with calcite as the main cementing material.

An attempt has been made here to study diagenetic imprints through isotopic changes in calcite cement, assemblage of clay minerals and abundance of K-feldspar in sandstones from Surai Khola section of Nepal Siwalik (Fig.2.1). Previous study from Surai Khola section showed interesting variation of carbon and oxygen isotope ratios of soil carbonate with implication of change in vegetation and climate during Miocene. It would be of interest to know how late diagenesis changed the pristine isotopic signature of sandstone cements and the mineralogy of sandstones. Such analysis is possible in case of Surai Khola due to availability of isotopic results from soil carbonates, which are less

susceptible to change and provide a well-constrained contemporary reference data set for comparison.

## 7.2 Cement morphology of sandstone

The primary cementing material of Siwalik sandstone is calcite. According to Tandon and Varshney (1991) calcite precipitated in sub-aerial vadoze zone due to capillary action under wet and dry climatic condition. Calcite in sandstone generally occurs as pore-filling variety with a patchy distribution (Fig.7.1a). Corrosion of quartz and feldspar grains by cementing action is common (Fig.7.1b, 1c). Calcite spar frequently shows complex variations in the birefringence colors indicating partial dissolution of crystals.

## 7.3 Isotopic Results

The  $\delta^{18}\text{O}$  values of sandstone cement samples show three evolutionary phases (Fig.7.2a). From 12 Ma to ~6 Ma, the average  $\delta^{18}\text{O}$  is around  $-13.6 \pm 1.9$  ‰ (n=114) with a large spread from  $-10$  to  $-18$  ‰. Subsequent to 6 Ma,  $\delta^{18}\text{O}$  shows sudden swing toward enriched values with less scatter in data; this enrichment continues up to 4 Ma. The average  $\delta^{18}\text{O}$  value for this time range is  $-10.7 \pm 1.6$  ‰ (n=25). Around 4 Ma, the  $\delta^{18}\text{O}$  reaches a maximum value of  $-7$  ‰. From 4 Ma to 2 Ma,  $\delta^{18}\text{O}$  value is fairly uniform with an average of  $-8.8 \pm 1.2$  ‰ (n=17) (Table 7.1).

Unlike  $\delta^{18}\text{O}$ , the  $\delta^{13}\text{C}$  of calcite cement does not show any definite trend with time (Fig.7.3) but varies randomly from  $-2.8$  ‰ to  $-9.9$  ‰. From 12 Ma to 7 Ma, the  $\delta^{13}\text{C}$  ranges between  $-3.3$  ‰ to  $-9.9$  ‰ with an average of  $-7.1 \pm 1.5$  ‰ (n=91). Subsequent to 7 Ma, the number of relatively enriched values increases. From 7 Ma to 2 Ma, the  $\delta^{13}\text{C}$  varies from  $-2.8$  ‰ to  $-9.2$  ‰ with an average of  $-5.7 \pm 1.5$  ‰ (n=65) (Table 7.1).

## 7.4 Discussion

### 7.4.1 Oxygen isotope ratio of carbonate cement

Oxygen isotope ratio of calcium carbonate depends on temperature of crystallization and oxygen isotope ratio of ambient water. Calcium carbonate precipitating at shallow level reflects the oxygen isotope ratio of local ground water initially but subsequent burial of the carbonate can modify this ratio.  $\delta^{18}\text{O}$  of carbonate associated with the sandstone bears the imprints of burial as discussed below.

**Temperature during burial:** Isotopic exchange between carbonate and fluid is not significant at temperatures typical of sedimentary environment except during dissolution and re-precipitation (Anderson, 1969; Land, 1980). Oxygen isotope exchange resulting from re-crystallization becomes more important as temperature rises. Since rise in temperature results in more negative  $\delta^{18}\text{O}$ , the most depleted value in a set of samples should represent the highest temperature acquired during burial. To calculate temperature of diagenesis from  $\delta^{18}\text{O}$  value of carbonate cement, oxygen isotopic composition of solution from which calcium carbonate has precipitated needs to be known. A critical but reasonable assumption about the  $\delta^{18}\text{O}$  value of formation water can be made from two inputs:  $\delta^{18}\text{O}$  of soil carbonate of same time period and modern day  $\delta^{18}\text{O}$  of meteoric water (ground water). The average oxygen isotope ratio of soil carbonate from Surai Khola section showed that pre-6 Ma (12 Ma to 6 Ma) meteoric water was depleted by  $\sim 3.5\%$  compared to the present day  $\delta^{18}\text{O}$  (Quade et al., 1995). Assuming that  $\delta^{18}\text{O}$  of shallow ground water is governed mostly by meteoric water (Krishnamurthy and Bhattacharya, 1991) and present day mean  $\delta^{18}\text{O}$  value of ground water on the piedmont of Nepal is  $-6.5\%$  (SMOW), (Quade et al., 1995) the  $\delta^{18}\text{O}$  of ground water for the time range 12 to 6 Ma can be approximately taken as  $-10\%$  (SMOW). Using this value of water  $\delta^{18}\text{O}$  and the Friedman-O'Neil (1977) equation of carbonate-water fractionation  $1000\ln\alpha_{\text{water}}^{\text{calcite}} = 2.78 \times 10^6 / T^2 - 2.89$  where  $\alpha_{\text{water}}^{\text{calcite}} = (1000 + \delta^{18}\text{O}_{\text{calcite}})/(1000 + \delta^{18}\text{O}_{\text{water}})$  it can be shown that the required temperature to achieve the most negative  $\delta^{18}\text{O}$  ( $-18\%$ ) is around  $57^\circ\text{C}$ . Such high value was possibly attained during deep burial of sediments (3 to 5 km).

Large scatter in  $\delta^{18}\text{O}$  values (from  $-10\%$  to  $-18\%$ ) at the bottom (12 to 10 Ma) of the stratigraphic succession may be due to dissolution and re-precipitation of calcites at different temperatures corresponding to various depths and generations during burial. As mentioned before, at a given level, the most negative  $\delta^{18}\text{O}$  probably represents calcite samples which precipitated at the highest available burial temperature; similarly, the most enriched  $^{18}\text{O}$  probably represents calcite precipitated at lowest

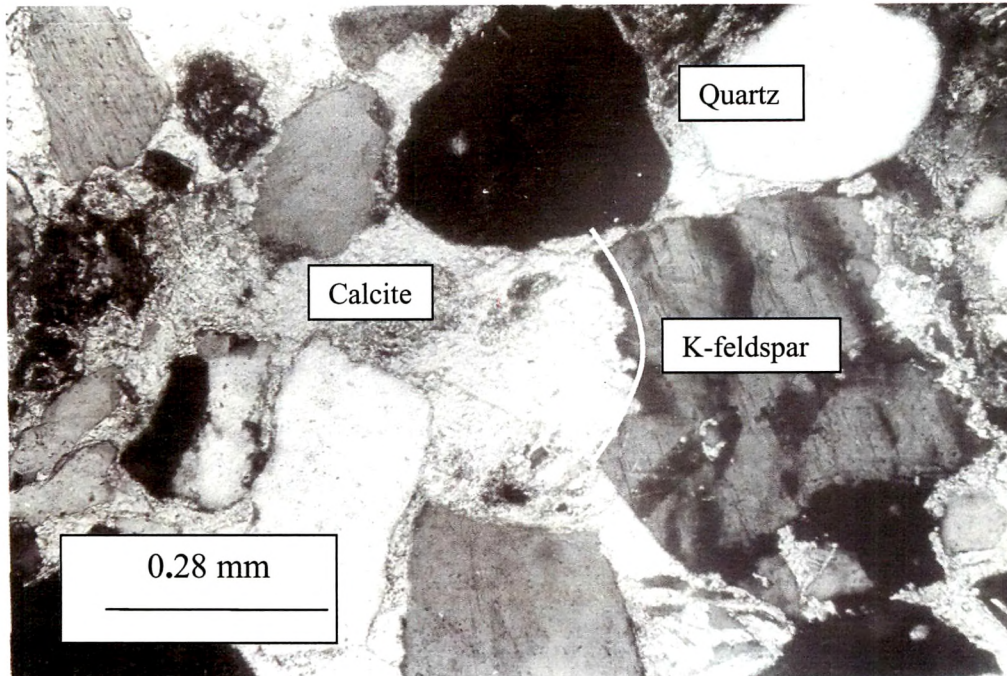


**Fig.7.1a** Thin section showing calcite cement filling the pore space of sandstone samples from Surai Khola. Dissolution of grain boundary (marked by white line) of K-feldspar grain by calcite cement is also shown.

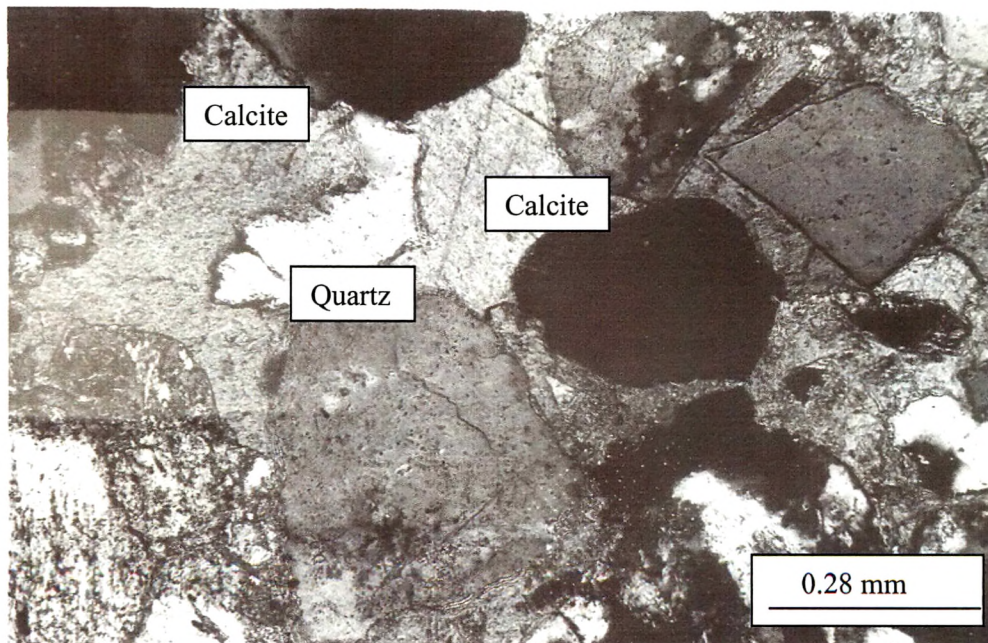


**Fig.7.1b** Remnant of quartz grain after corrosion by calcite cement in medium grained sandstone

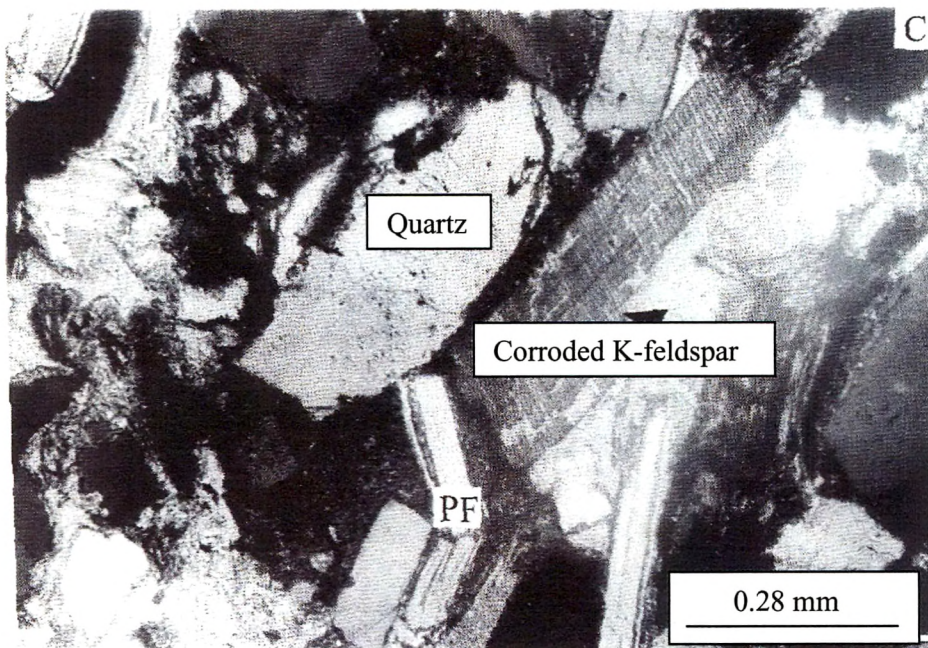


**Fig.7.1c** Corrosion of K-feldspar grain by calcite cement.

obtainable temperature (assuming  $\delta^{18}\text{O}$  of formation water is same for both samples since they are from the same level). At around 11.6 Ma, the maximum and minimum  $\delta^{18}\text{O}$  are  $-10\text{‰}$  and  $-18\text{‰}$  respectively; these values correspond to a temperature difference of  $40^\circ\text{C}$  for calcite precipitation between these two samples (calculated using Friedman-O'Neil equation where the  $\delta^{18}\text{O}$  of water has been taken as  $-10\text{‰}$ ) where the depleted  $^{18}\text{O}$  represents precipitation at greater depth compared to the enriched  $^{18}\text{O}$  sample. It is conceivable that the depth of calcite precipitation varied due to syn-depositional nature of the Siwalik basin where continuous sedimentation was associated with subsidence and burial of older sediments under younger sediments. During this descent, isotopic ratio of cement could have changed due to dissolution/re-precipitation of calcite. However, some samples suffered minimal change and some probably retained the original isotopic signature. This implies that the depleted value is most altered and the enriched value is least altered when samples are compared at the same stratigraphic

**Table.7.1** Carbon and oxygen isotope ratio of carbonate cement from sandstone

Sample No	Age(Ma)	$\delta^{13}\text{C}$	$\delta^{18}\text{O}$	Sample No	Age (Ma)	$\delta^{13}\text{C}$	$\delta^{18}\text{O}$
PS2K-BNK-02-S1	12.0	-7.2	-17.6	PS2K-BNK-48-S14	10.5	-8.2	-11.8
PS2K-BNK-04-S2	12.0	-9.2	-16.5	PS2K-BNK-48-S15	10.5	-8.2	-16.3
PS2K-BNK-07-S2	11.9	-9.8	-11.1	PS2K-BNK-48-S19	10.5	-6.7	-14.6
PS2K-BNK-08-S2	11.9	-7.6	-15.7	PS2K-BNK-49-S2	10.5	-7.8	-11.7
PS2K-BNK-10-S1	11.9	-7.2	-15.5	PS2K-BNK-50-S1	10.5	-8.2	-12.1
PS2K-BNK-012S1	11.9	-8.5	-15.0	PS2K-BNK-51-S1	10.4	-5.7	-14.5
PS2K-BNK-012S2	11.7	-6.7	-15.7	PS2K-BNK-51-S3	10.4	-5.3	-15.3
PS2K-BNK-15-S3	11.7	-7.5	-11.4	PS2K-BNK-52-S2	10.4	-6.9	-13.4
PS2K-BNK-15-S4	11.7	-7.7	-11.7	PS2K-BNK-54-S2	10.4	-5.3	-13.2
PS2K-BNK-20-S2	11.7	-8.1	-14.0	PS2K-BNK-55-S1	10.4	-5.7	-13.3
PS2K-BNK-22-S1	11.7	-9.6	-10.4	PS2K-BNK-59-S2	10.3	-6.8	-12.6
PS2K-BNK-22-S2	11.7	-8.7	-10.0	PS2K-BNK-61-S1	10.3	-6.0	-15.9
PS2K-BNK-25S2	11.6	-5.6	-15.7	PS2K-BNK-62-S1	10.3	-8.3	-10.7
PS2K-BNK-26-S2	11.6	-5.3	-13.5	PS2K-BNK-66-S2	10.1	-6.9	-12.6
PS2K-BNK-27-S2	11.6	-5.3	-13.3	PS2K-BNK-67-S2	10.0	-8.6	-17.5
PS2K-BNK-27S2(R)	11.5	-6.3	-14.9	PS2K-BNK-68-S1	9.9	-8.3	-16.3
PS2K-BNK-28-S2	11.2	-6.6	-12.1	PS2K-BNK-68-S2	9.8	-8.4	-18.0
PS2K-BNK-30-S2	11.2	-6.7	-12.2	PS2K-BNK-69-S1	9.7	-8.6	-17.3
PS2K-BNK-32-S1	11.1	-8.3	-15.2	PS2K-BNK-69-S2	9.6	-7.5	-15.1
PS2K-BNK-34-S2	11.1	-8.1	-11.5	PS2K-BNK-70-S2	9.5	-5.4	-13.7
PS2K-BNK-36-S2	11.0	-6.5	-16.2	PS2K-BNK-71-S1	9.4	-9.2	-10.7
PS2K-BNK-37-S1	10.7	-5.5	-12.7	PS2K-BNK-72-S2	9.2	-8.6	-12.5
PS2K-BNK-42-S2	10.7	-5.8	-13.8	PS2K-BNK-77-S2	9.1	-5.0	-15.7
PS2K-BNK-44-S1	10.7	-9.6	-11.0	PS2K-BNK-80-S2	9.1	-5.9	-10.7
PS2K-BNK-45-S1	10.7	-9.5	-11.7	PS2K-BNK-81-S2	9.1	-5.6	-12.5
PS2K-BNK-45-S2	10.6	-9.0	-17.7	PS2K-BNK-86-S1	9.0	-6.6	-14.7
PS2K-BNK-48-S1	10.6	-5.5	-12.6	PS2K-BNK-86-S2	9.0	-8.7	-10.3
PS2K-BNK-48-S2	10.6	-5.7	-14.4	PS2K-BNK-87-S1	8.5	-8.6	-11.3
PS2K-BNK-48-S4	10.6	-6.8	-15.4	PS2K-BNK-92-S2	8.2	-6.1	-16.5
PS2K-BNK-48-S6	10.6	-7.2	-16.1	PS2K-SK-114-S	8.0	-6.0	-16.4
PS2K-BNK-48-S10	10.6	-5.3	-11.7	PS2K-SK-114-S	8.0	-6.8	-12.4
PS2K-BNK-48-S11	10.5	-6.0	-12.9	PS2K-SK-117-S1	8.0	-7.7	-11.4
PS2K-BNK-48-S13	10.5	-9.3	-10.1	PS2K-SK-121-S1	7.9	-6.9	-15.5

Sample No	Age(Ma)	$\delta^{13}\text{C}$	$\delta^{18}\text{O}$	Sample No	Age(Ma)	$\delta^{13}\text{C}$	$\delta^{18}\text{O}$
PS2K-SK-122-S2	7.9	-7.3	-13.3	PS2K-SK-210-S1	6.2	-4.6	-14.8
PS2K-SK-123-S2	7.9	-8.8	-11.1	PS2K-SK-215-S1	6.2	-4.7	-14.5
PS2K-SK-123-S1	7.9	-6.9	-14.7	PS2K-SK-216-S1	6.2	-4.9	-13.1
PS2K-SK-125-S1	7.8	-7.9	-12.5	PS2K-SK-217-S1	6.2	-7.1	-16.8
PS2K-SK-129-S1	7.8	-5.0	-15.6	PS2K-SK-218-S1	6.1	-4.7	-13.8
PS2K-SK-133-S1	7.8	-8.9	-11.9	PS2K-SK-219-S1	6.1	-3.8	-13.8
PS2K-SK-133-S2	7.7	-8.4	-11.3	PS2K-SK-222-S1	6.1	-4.8	-12.4
PS2K-SK-134-S2	7.7	-6.1	-12.3	PS2K-SK-223-S1	6.1	-3.7	-13.6
PS2K-SK-137-S1	7.7	-6.1	-12.9	PS2K-SK-224-S1	6.1	-4.4	-12.0
PS2K-SK-137-S1	7.6	-7.8	-12.6	PS2K-SK-224-S2	6.1	-3.9	-12.0
PS2K-SK-138-S1	7.6	-7.7	-13.4	PS2K-SK-225-S1	6.0	-4.2	-12.9
PS2K-SK-138-S2	7.6	-9.2	-11.6	PS2K-SK-229-S1	6.0	-4.4	-11.4
PS2K-SK-139-S1	7.5	-3.3	-13.3	PS2K-SK-229-S2	5.4	-4.6	-10.6
PS2K-SK-142-S1	7.4	-5.7	-14.5	PS2K-SK-242-S1	5.4	-7.8	-11.5
PS2K-SK-153-S2	7.3	-8.8	-13.9	PS2K-SK-242-S2	5.3	-4.4	-12.8
PS2K-SK-154-S2	7.3	-4.0	-15.5	PS2K-SK-244-S1	5.3	-3.0	-13.6
PS2K-SK-155-S2	7.3	-7.1	-12.3	PS2K-SK-245-S1	5.2	-8.9	-10.9
PS2K-SK-156-S1	7.3	-6.5	-13.1	PS2K-SK-247-S1	5.1	-5.6	-10.6
PS2K-SK-156-S2	7.2	-5.6	-12.9	PS2K-SK-253-S1	5.1	-6.2	-10.7
PS2K-SK-159-S2	7.2	-6.6	-11.9	PS2K-SK-255-S1	4.9	-3.6	-13.4
PS2K-SK-159-S1	7.1	-9.4	-12.7	PS2K-DB-270-S1	4.8	-6.3	-10.4
PS2K-SK-160-S1	7.1	-8.9	-12.2	PS2K-DB-271-S1	4.7	-8.1	-10.9
PS2K-SK-160-S2	7.1	-6.4	-12.3	PS2K-DB-275-S1	4.7	-7.9	-10.9
PS2K-SK-163-S2	7.1	-8.3	-15.4	PS2K-DB-275-S2	4.7	-8.8	-10.8
PS2K-SK-163-S4	7.0	-3.5	-15.4	PS2K-DB-276-S2	4.7	-6.5	-8.8
PS2K-SK-166-S1	6.5	-5.0	-14.4	PS2K-DB-280-S1	4.7	-7.5	-8.1
PS2K-SK-172-S1	6.4	-5.1	-12.2	PS2K-DB-280-S2	4.7	-7.8	-10.1
PS2K-SK-183-S1	6.4	-7.2	-14.5	PS2K-DB-280-S4	4.6	-5.3	-11.1
PS2K-SK-194-S1	6.4	-5.4	-13.6	PS2K-DB-285-S1	4.6	-9.2	-9.2
PS2K-SK-196-S1	6.4	-5.9	-14.6	PS2K-DB-285-S2	4.5	-5.9	-8.5
PS2K-SK-199-S1	6.4	-5.5	-13.2	PS2K-DB-287-S1	4.5	-5.5	-9.6
PS2K-SK-199-S2	6.4	-5.2	-13.7	PS2K-DB-287-S2	4.5	-3.9	-12.5
PS2K-SK-199-S2	6.3	-5.1	-12.7	PS2K-DB-288-S1	4.5	-5.2	-7.9
PS2K-SK-203-S1	6.3	-3.9	-12.2	PS2K-DB-289-S1	4.4	-5.1	-8.0
PS2K-SK-204-S1	6.3	-6.0	-13.6	PS2K-DB-290-S1	4.4	-7.6	-12.1
PS2K-SK-206-S1	6.3	-5.8	-12.2	PS2K-DB-295-S1	3.9	-5.3	-10.9
PS2K-SK-209-S1	6.2	-4.7	-14.2	PS2K-DB-320-S1	3.9	-6.3	-8.7

Sample No	Age (Ma)	$\delta^{13}\text{C}$	$\delta^{18}\text{O}$	Sample No	Age (Ma)	$\delta^{13}\text{C}$	$\delta^{18}\text{O}$
PS2K-DB-320-S2	3.86	-2.8	-10.9	PS2K-DB-329-S2	3.7	-5.8	-8.5
PS2K-DB-321-S1	3.85	-8.6	-7.8	PS2K-DB-331-S1	3.7	-6.7	-7.7
PS2K-DB-322-S1	3.83	-7.7	-9.2	PS2K-DB-334-S1	3.0	-6.3	-7.8
PS2K-DB-323-S1	3.83	-7.4	-8.9	PS2K-DB-373-S1	3.0	-6.5	-7.9
PS2K-DB-323-S2	3.79	-4.5	-10.9	PS2K-DB-373-S2	2.9	-5.3	-7.5
PS2K-DB-326-S1	3.79	-5.4	-8.3	PS2K-DB-377-S1	2.5	-5.4	-8.6
PS2K-DB-326-S2	3.73	-4.5	-9.3	PS2K-DN-389-S1	2.5	-6.8	-7.7
PS2K-DB-329-S1	3.73	-2.6	-8.1				

level. We further assume that the least altered value corresponds to calcite deposition near the surface level of the sediment column. Using this assumption, the maximum depth up to which re-precipitation of cement could have taken place can be estimated from the temperature difference between the most enriched and most depleted values from same stratigraphic level. Using the observed geothermal gradient of the Siwalik basin  $\sim 20^\circ\text{C}/\text{km}$  (Mugnier et al., 1995) and assuming that the initial  $\delta^{18}\text{O}$  was same for both the samples  $40^\circ\text{C}$  difference in temperature requires at least 2 km subsidence.

With decrease in depth, the scatter in  $\delta^{18}\text{O}$  decreases. At around 7.5 Ma, the most depleted value is  $-15.6\text{‰}$  and the most enriched value is  $-10\text{‰}$ . The temperature difference of precipitation for these two samples is  $28^\circ\text{C}$  ( $44^\circ\text{C}$  for  $-15.6\text{‰}$  and  $16^\circ\text{C}$  for  $-10\text{‰}$ ) which implies a burial of  $\sim 1.5$  km. The decrease in temperature difference with decrease in stratigraphic depth supports our assumption that temperature was the main controlling factor for oxygen isotope alteration in calcite cement.

The maximum depth up to which re-precipitation and re-crystallization has occurred can also be calculated from the most depleted value at a given stratigraphic level (S.L.) as it corresponds to maximum temperature acquired during burial. The maximum temperatures estimated in this way for 11.6 Ma (S.L.=4.9 km) and 7.5 Ma (S.L. =3.5 km) are  $57^\circ\text{C}$  and  $44^\circ\text{C}$  respectively corresponding to burial depths of nearly 2 km and 1.5 km (taking surface temperature as  $16^\circ\text{C}$  corresponding to  $-10\text{‰}$  value obtained near the sediment surface as discussed above.). Near agreement of calculated depths for re-precipitation of calcite from horizontal spread of  $\delta^{18}\text{O}$  and from most

depleted values at a given S.L. supports our contention that re-precipitation of calcite below 2 km was not significant.

This estimate of depth may represent a lower limit as re-precipitation of calcite is also possible during the uplift. The Siwalik basin was about 5.5 km deep and as

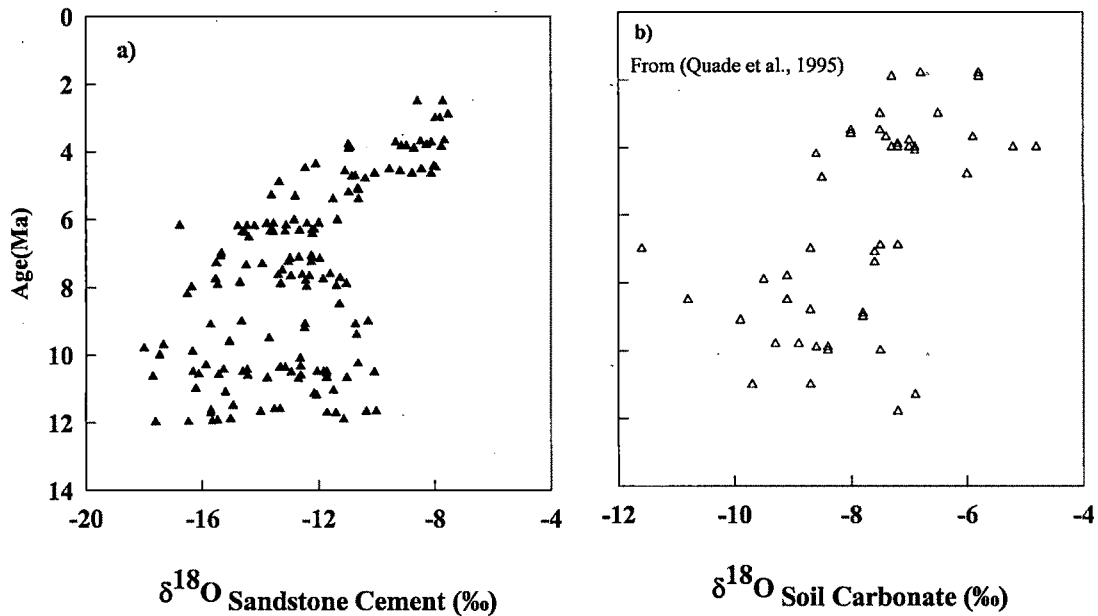


**Fig.7.2** a) Oxygen isotope ratio of diagenetic calcite cement from sandstone samples of Surai Khola showing three evolutionary phases. From 12 Ma to 6 Ma, oxygen isotope ratio is characterized by large spread:  $-10$  to  $-18$  ‰. The large spread is probably due to dissolution and re-precipitation of carbonate at different stages of burial. At around 6 Ma, the  $^{18}\text{O}$  shows sudden swing towards enriched values and the maximum enrichment is attained near 4 Ma. The sudden swing is in tandem with enrichment of oxygen isotope ratio in soil carbonate (Fig. 2b; Data from Quade et al., 1995) from the same section, which indicates change in precipitational pattern. The similar trend of isotope ratio for cement and soil carbonate (for post 6 Ma period) suggests meteoric water has played an important role in determining the ratio during diagenesis. However, the ratio of sandstone cement is depleted compared to the ratio of soil carbonate (b). The depletion may be due to precipitation of cement at higher temperature compared to that of soil carbonate. Subsequent to 4 Ma, the  $\delta^{18}\text{O}$  is nearly constant.

mentioned before, this depth was achieved due to continuous sinking during sedimentation. Later, as a result of tectonic activity, sediment in the foreland basin got uplifted. New generation of calcite could have precipitated during the upliftment at relatively lower temperature. The  $\delta^{18}\text{O}$  of this generation of calcite would be enriched

compared to the calcite precipitated at higher depth. Thus, it is possible that the calculated depth of re-precipitation underestimates the actual depth of burial for samples which experienced subsidence followed by uplift.

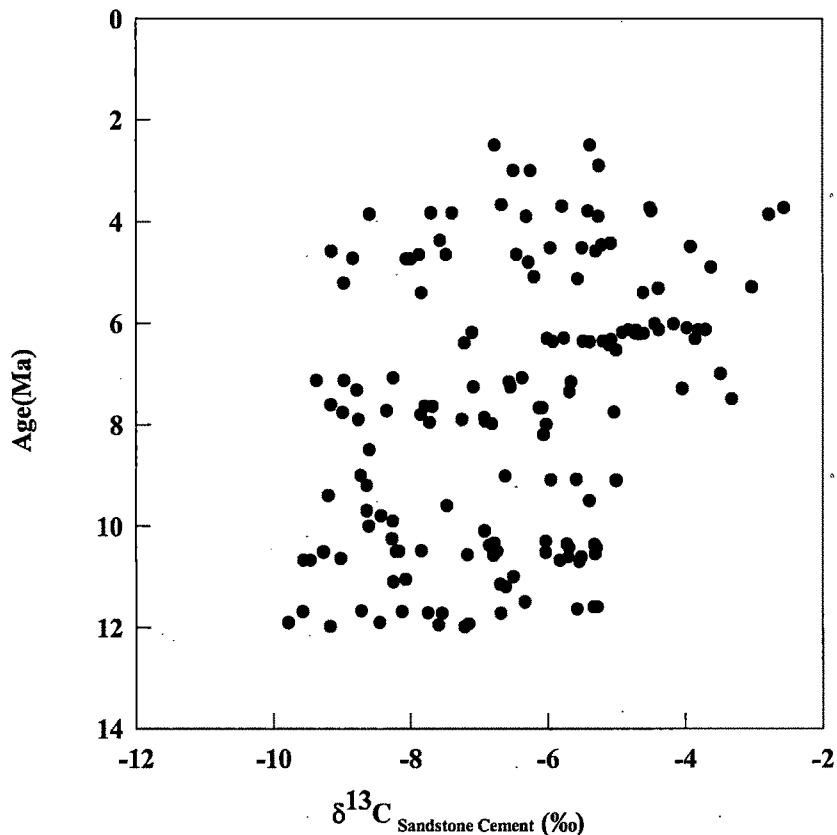


**Fig.7.3** Carbon isotope ratio of carbonate cement from sandstone shows large spread throughout the section. From 12 Ma to 7 Ma the  $\delta^{13}C$  ranges between  $-3.3$  to  $-9.9$  ‰ with an average of  $-7.1 \pm 1.5$  ‰ ( $n=91$ ) and the post 7 Ma time the  $\delta^{13}C$  ranges from  $-2.8$  to  $-9.2$  ‰ with an average of  $-5.7 \pm 1.5$  ‰ ( $n=65$ ).  $CO_2$  produced from decomposition of organic matter at various stages of burial and dissolution and re-precipitation of carbonate could be the cause of large spread in the carbon isotope ratio of carbonate. The enrichment in the carbon isotope ratio subsequent to 7 Ma probably reflects appearance of  $C_4$  plants in the flood plain, which has enriched carbon isotope ratio compared to the  $C_3$  plants.

During diagenesis, with increase in depth, dissolution and re-precipitation of minerals prone to diagenesis increase. Several workers suggested that alkali feldspar

undergoes extensive dissolution during burial diagenesis of sandstone (Milliken, 1989; Harris, 1992; Wilkinson and Haszeldine, 1996). Thin section analysis of Surai Khola sandstone shows absence of K-feldspars in the older samples in most cases while in the younger samples, K-feldspar is present with corrosive features (Fig.7.1a, 1c). Dissolution of K-feldspar is probably the result of interaction with weakly acidic pore fluid formed by decomposition of organic matter. Dissolution of K-feldspar results in increasing concentration of K, Al and SiO<sub>2</sub> in the diagenetic fluid, which can cause precipitation of quartz and illite. The semi-quantitative analysis of clays shows increase in abundance of illite with increase in stratigraphic depth, consistent with above observation.

**Role of diagenetic fluid:** Calcite cementation in fluvial sandstone probably occurs in shallow ground water regime due to capillary evaporation. It has been shown that oxygen isotope ratio of early diagenetic carbonate cement in sandstone represents ground water oxygen isotope ratio (Sanyal et al., 2004b) which, in turn, is mainly determined by the oxygen isotope ratio of meteoric water as it recharges the ground water with little or no fractionation. Any carbonate precipitating in equilibrium with ground water would reflect the oxygen isotope ratio of ground water as long as the carbonate does not interact with other sources. As discussed earlier, scattered  $\delta^{18}\text{O}$  values of carbonate cement in lower part of the stratigraphic section at Surai Khola (pre-6 Ma period) indicate dissolution and re-precipitation of carbonate during deep burial. At around 6 Ma, the scatter in  $\delta^{18}\text{O}$  decreases on either side (both enriched and depleted side) resulting in a conical shape of depth variation. The increase in depleted side values indicates lowering of temperature of re-precipitation while decrease in the enriched side may indicate change in the isotopic composition of water. Subsequent to 6 Ma, the  $\delta^{18}\text{O}$  of carbonate cement increases rapidly, which is in accordance with the observed enrichment of  $^{18}\text{O}$  of soil carbonate in Surai Khola section (Fig.7.2b) (Quade et al., 1995) and other sections of Indian Siwalik (Sanyal et al., 2004a). The profile of  $\delta^{18}\text{O}$  variation by considering only the most enriched values shows a minimum at around 6 Ma, which compares well with the proposed intensification of monsoon in Indian sub-continent based on pedogenic carbonate (Sanyal et al., 2004a). This indicates that despite alteration and consequent scatter, signature of a rapid  $\delta^{18}\text{O}$  change is still

preserved in the sandstone. Additionally, it establishes that the  $\delta^{18}\text{O}$  signal is definitely induced by meteoric water and represents a significant regional change in the rainfall pattern.

It is to be noted that  $^{18}\text{O}/^{16}\text{O}$  ratio in sandstone cement is generally depleted compared to that of soil carbonate at the same stratigraphic depth despite having a similar trend in depth variation. This probably indicates higher formation temperature of sandstone calcite. Depleted oxygen isotope ratio in sandstone cement can also be caused by mixing of river water with shallow ground water by lateral flow. In the Himalayan region, river water flowing from highlands has lower  $\delta^{18}\text{O}$  values than the water from low land. Mixing between groundwater and the local river water would, therefore, make the  $\delta^{18}\text{O}$  value of formation water more depleted.

Detrital carbonates can, in principle, contribute to the bulk carbonate. The Siwalik sediments are weathering products of Himalayan rocks, which have many limestone formations. The  $\delta^{18}\text{O}$  value of Himalayan marine limestones ranges from  $-8.9$  to  $-14.5\text{‰}$  (Quade et al., 1995). Contribution from such carbonates can make  $\delta^{18}\text{O}$  of bulk carbonate more negative compared to carbonates precipitated from groundwater. However, modal abundance of carbonate grains shows only 2% to 15% of the carbonate as detrital. The contribution of detrital carbonate to the bulk  $\delta^{18}\text{O}$  in various time brackets can be calculated by isotopic mass balance using the following inputs: (i) average bulk  $\delta^{18}\text{O}$  values: for 12 to 6 Ma,  $-13.6\text{‰}$ ; for 6 to 4 Ma,  $-10.7\text{‰}$ ; and for 4 to 2 Ma,  $-8.8\text{‰}$  (ii) average  $\delta^{18}\text{O}$  of detrital carbonate as:  $-11.7\text{‰}$  from the observed range  $-8.9$  to  $-14.5\text{‰}$  (Quade et al., 1995) (iii) abundance of the detrital carbonate from 2 to 15%. Such calculation shows that maximum correction from detrital carbonate contribution is  $-0.3\text{‰}$  for 12 to 6 Ma; for 6 to 4 Ma  $+0.2\text{‰}$ ; and for 4 to 2 Ma  $+0.5\text{‰}$ . This calculation indicates that the contribution of the detrital carbonate is not significant in changing the bulk  $\delta^{18}\text{O}$ , especially in view of the large scatter introduced by several other factors discussed before.

We, therefore, conclude that in the lower part of the stratigraphic section the large scatter is due to re-precipitation of calcite at different stages during burial and uplift and subsequent to 6 Ma, the oxygen isotope ratio of calcite is mainly controlled by meteoric water.

### 7.5 Carbon isotope ratio of carbonate cement of sandstone

In general, the dissolved inorganic carbon in shallow groundwater below the soil zone is in isotopic equilibrium with plant-derived CO<sub>2</sub> if the soil has substantial vegetation (Pearson and Hanshaw, 1970; Fritz et al., 1978; Bath et al., 1979; Deak, 1979; Andrews et al., 1984; Wassennar et al., 1992; Leaney and Herczeg, 1995; Clark et al., 1997). Ground water calcite should also form in equilibrium with this reservoir as long as it forms shortly after burial and does not undergo extensive interaction with carbon sources other than plant-derived CO<sub>2</sub>.

Plant-derived CO<sub>2</sub> can have different  $\delta^{13}\text{C}$  values depending on the type of plant since different plants have different photosynthetic pathway. The majority of plants, comprising trees, shrubs, cool-season grasses etc., follow the C<sub>3</sub> pathway. The  $\delta^{13}\text{C}$  of C<sub>3</sub> plants vary over a large range: -20 to -35 ‰ but the average is well constrained at -26.7 ‰. For the C<sub>4</sub> type of plants (grasses),  $\delta^{13}\text{C}$  values range from -6 ‰ to -19 ‰, with an average of about -13 ‰ (Cerling et al., 1997). When calcium carbonate forms in equilibrium with plant-derived CO<sub>2</sub>, the  $\delta^{13}\text{C}$  of calcium carbonate become enriched by 14 to 17 ‰ compared to the plant-derived CO<sub>2</sub> depending on temperature (Cerling, 1984).

Vegetational reconstruction based on carbon isotope ratio of soil carbonate from Surai Khola section showed that the flood plain in pre-7 Ma time was dominated by C<sub>3</sub> type of plants (Quade et al., 1995). Therefore, sandstone carbonates older than 7 Ma and precipitating from shallow ground water should have values around -10 to -13‰ depending on the temperature of precipitation. However, this is not observed in the data set. Instead, there is a large scatter from -10 to -5 ‰ indicating other sources of carbon. As discussed earlier, the scatter in oxygen isotope ratio of the cement indicates dissolution and re-precipitation of carbonate during burial and uplift. The same effects can lead to carbon isotope ratio variation. During progress of diagenesis associated with burial, organic matter contained in sandstone undergoes several decarbonation reactions and CO<sub>2</sub> produced from these reactions can have different isotopic ratios. With progress in burial, organic matter gets modified by processes like fermentation, thermally induced decarboxylation etc. operating at different depths (Irwin et al., 1977). Carbon isotope ratio of CO<sub>2</sub> produced during these reactions can vary from -25‰ to +15‰. At the

highest level of diagenesis, thermal decomposition of organic matter can produce very depleted CO<sub>2</sub> (–25 ‰) whereas fermentation can produce very enriched CO<sub>2</sub> (+15 ‰). Large spread of carbon isotope ratio at the same stratigraphic level probably indicates precipitation of carbonate in equilibrium with CO<sub>2</sub> derived from plant organic matter but at various stages of decarbonation.

Subsequent to 7 Ma, the spread in δ<sup>13</sup>C values increases. Interestingly, enriched carbon isotope ratios (up to –2.5‰) also appear (Fig.7.3). The enriched values are possibly due to appearance and expansion of C<sub>4</sub> plants in the flood plain, a fact known from earlier studies (Quade et al., 1995). Carbon isotope ratio of soil carbonate from Surai Khola section showed decrease in abundance of C<sub>3</sub> plants and expansion of C<sub>4</sub> plants in the flood plain at around 7 Ma (Quade et al., 1995). Larger spread in carbon isotope ratio for post-7 Ma period may be due to incorporation of organic matter from upper reaches by lateral flow of river water into ground water. In such circumstances, carbon isotope ratio of cement represents not only the vegetation of flood plain but also the vegetation of the catchment area. Organic matter brought from higher reaches would have C<sub>3</sub> type δ<sup>13</sup>C value. Depending on the mixing between the in-situ CO<sub>2</sub> and CO<sub>2</sub> produced from oxidation of transported organic matter the carbon isotope ratio of the cement would vary. For pre-7 Ma time period, this factor did not play significant role as both in the flood plain and higher reaches the vegetation was of C<sub>3</sub> type.

### **7.6 Clay mineral assemblage in sandstone**

Sediments in the Siwalik foreland basin are weathering products of rocks derived from one of the most tectonically active areas in the world i.e. the Himalaya. Weathered materials are being transported to the foreland basin from the Higher, Lesser and Sub-Himalaya (Kumar et al., 1999; Ghosh et al., 2003) for last 18 Myr. Weathering of these rocks is accompanied by varying degrees of dissolution and in-situ precipitation of authigenic products, of which clay minerals are a major component. Higher Himalayan rocks have large percentage of granitic rocks, which are prone to produce illite and chlorite rich clays, whereas lesser Himalayan hinterland volcanic rocks mainly produce smectite. Kaolinite can also form from lesser Himalayan rocks during chemical weathering in warm temperature, but develops principally in climate that have wet and

dry seasons and have more water percolation than that needed for smectite formation (Suresh et al., 2004).

Less than 2-micron grains separated from sandstone show presence of smectite, kaolinite, chlorite and illite clay minerals (Fig.7.4). Semi-quantitative estimation of the

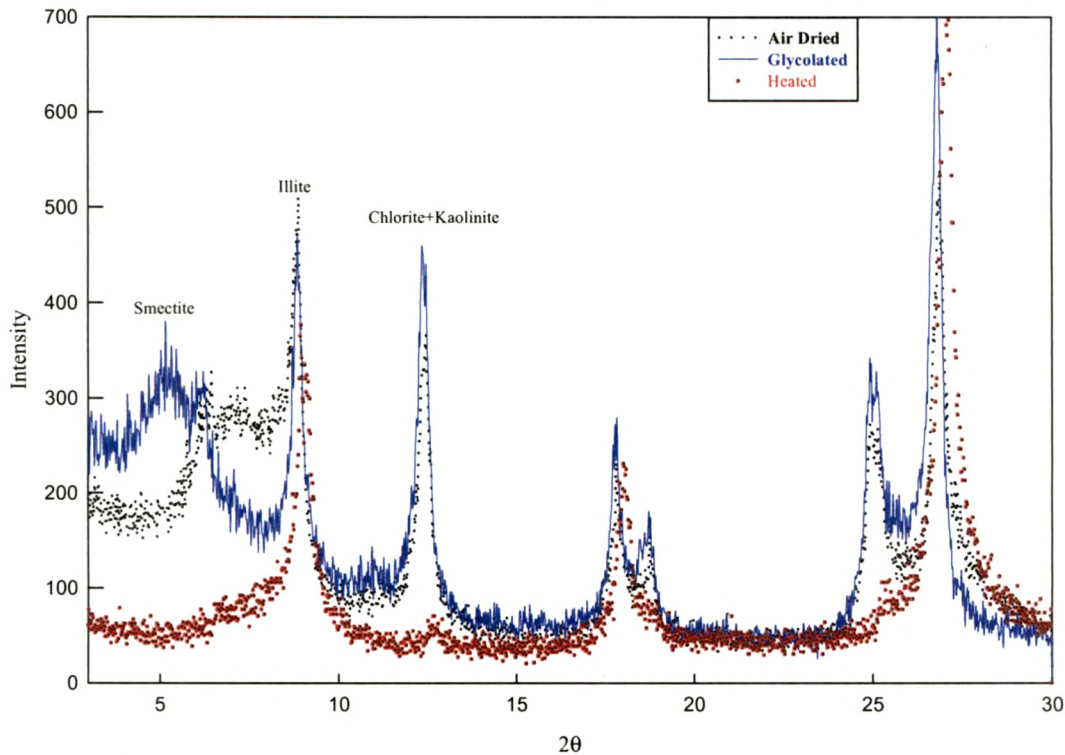


**Fig.7.4** X-ray diffraction pattern of less than 2 micron size clay minerals separated from Surai Khola sandstone. Glycolation of oriented slide shows shifting of air-dried  $6.2^\circ$   $2\theta$  peak to  $5.1^\circ$   $2\theta$  confirming the presence of smectite.  $8.8^\circ$  and  $12.4^\circ$   $2\theta$  peaks confirm the presence of illite and chlorite.  $24.9^\circ$  and  $25.1^\circ$  peaks confirm the presence of chlorite and kaolinite. Heating of clay slide up to  $550^\circ\text{C}$  shows disappearance of smectite, chlorite and kaolinite peaks

relative abundance of clay minerals was done based on the peak area method (Biscaye, 1965). The peak areas of glycolated samples were first computed under  $17\text{\AA}$  peak for smectite,  $10\text{\AA}$  peak for illite and  $7\text{\AA}$  peak for chlorite and kaolinite. These

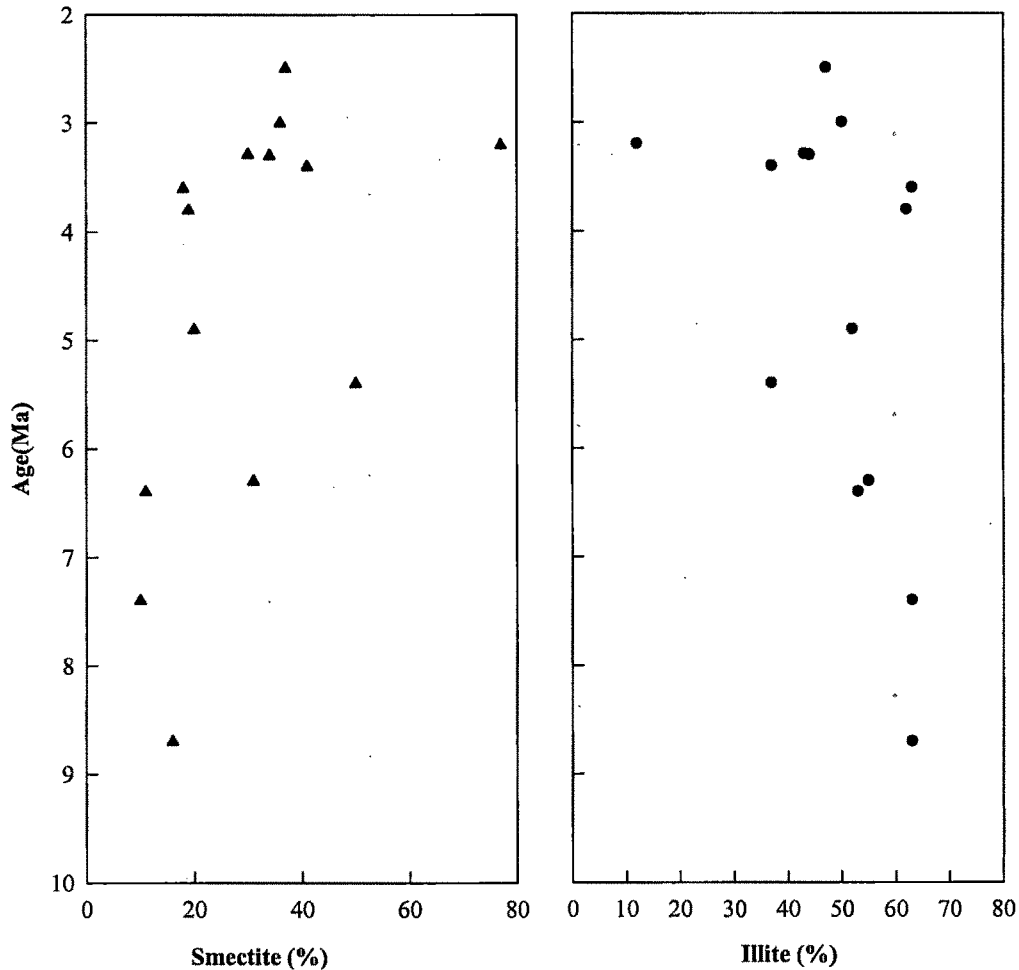


**Fig.7.5** Time variation of smectite and illite abundances from Surai Khola sandstone. The maximum abundance (63%) of illite is found in the lower part of the stratigraphic succession and minimum abundance (12%) is seen in the upper part. In contrast, the maximum abundance (70%) of smectite is found near the top of the section and the minimum abundance (10%) is found at lower part. Increase in the abundance of illite with increase in depth probably represents progressive illitization of smectite.

values were multiplied by the weighting factors 1, 4, 2 and 2 respectively, for smectite, illite, chlorite and kaolinite (Biscaye, 1965). The relative proportions of chlorite and kaolinite were determined from the ratio of peak heights (3.53 Å and 3.58 Å respectively) when this ratio is 1, the amount of chlorite is assumed to be twice that of kaolinite.

Semi-quantitative analysis of clays shows increase in abundance of illite and

decrease in smectite with increase in depth. (Fig.7.5). In the lower part of the stratigraphic succession the abundance of illite rose to a maximum of 63%, whereas, minimum abundance (12%) was found in the upper part. On the other hand, the maximum abundance (70%) of smectite was found near the top of the section and the minimum abundance (10%) was found at lower part. The difference in these abundances could be the result of progressive transformation of smectite into illite with increase in depth. During burial diagenesis, smectite transforms into illite due to loss of water molecules from crystal lattice (Keller, 1970). Progressive transformation of smectite to illite depends on time, potassium availability, water/rock ratio, fluid and rock composition, starting composition of mixed layer illite-smectite and pressure. Although clay distribution appears to be a function of depth, it is controlled primarily by temperature (Pollastro, 1989). On the whole, the clay mineral analysis supports the explanation regarding isotope changes caused by burial diagenesis.

### **7.7 Conclusions**

Isotopic imprints on diagenetic calcite cement shows that temperature and meteoric water played major role during diagenesis of Surai Khola sandstone. In the lower part of the succession (12 to 6 Ma) re-precipitation of successive generation of calcite at different temperatures was possibly responsible for variation of oxygen isotope ratio. The dissolution/re-precipitation seems to have been active up to depth of 2 km. With decrease in burial depth, the variation in oxygen isotope ratio decreases due to decrease in temperature. During the post-6 Ma period, along with temperature, meteoric water also played a major role in controlling the oxygen isotope ratio. The oxygen isotope ratio variation in cement of the post-6 Ma period shows that despite the complicating presence of diagenetic change it can still be used to decipher alteration in meteoric water isotopic composition due to monsoon variation.

Mineralogical abundance also shows significant change during diagenesis. The smectite abundance decreases with depth whereas illite abundance increases. With increase in depth, K-feldspar abundance also decreases along with illitization of smectite. Dissolution of K-feldspar might have supplied the potassium during illitization of smectite.